PROCEEDINGS OF SCIENCE

Results from the O3 observing run of the LIGO-Virgo Collaboration

Rosa Poggiani[*] [†] **on behalf of the LIGO Scientific Collaboration and the Virgo Collaboration**
Università di Pisa and Istituto Nazionale di Fisica Nucleare, Sezione di Pisa
E-mail: rosa.poggiani@unipi.it

The third observation run (O3) of Advanced LIGO and Advanced Virgo started in April 2019 and ended in March 2020, with improved sensitivities compared to the previous observing run. The paper will review the science results achieved during the O3 run, that include the catalogs of compact binary mergers and some exceptional events: GW190412, the merger of two black holes with asymmetric masses; GW190425, the second observed binary neutron star merger; GW190521, the first detection of an intermediate mass black hole; GW190814, a system with a secondary that could be either a black hole or a neutron star; GW200105 and GW200115, the first detected neutron star-black hole binary mergers. The impact of detections on astrophysics will also be reviewed.

*** *High Energy Astrophysics in Southern Africa (HEASA2021)* ***
*** *13 - 17 September, 2021* ***
*** *Online* ***

[*]Speaker.
[†]Corresponding author

PoS(HEASA2021)060

1. Introduction

Gravitational waves (GW) were firstly detected by the two Advanced LIGO interferometers in September 2015 during the first observing run (O1). The first detection, GW150914, was the merger of a binary black hole (BBH) system [1]. GW170817 [2], the first binary neutron star (BNS) merger was detected, together with its electromagnetic counterpart [3, 4], during the second observing run O2. The detections during O1 and O2 runs have been collected into GWTC-1, the First Gravitational Wave Transient Catalog [6]. The present review focuses on the LIGO-Virgo observations during the third observing run (O3), that started in April 2019 and ended in March 2020 because of the Covid-19 pandemic. The cumulative number of O1+O2+O3 candidates versus the effective surveyed time-volume for BNS mergers is shown in Fig. 1.

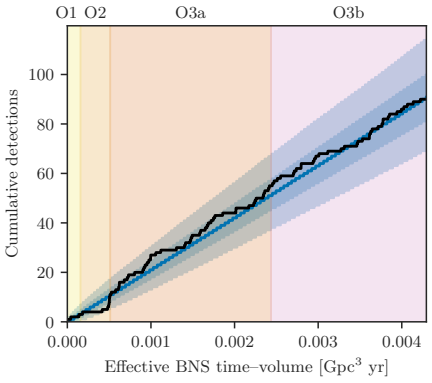

Figure 1: Candidate events with probability of astrophysical origin $p_{astro} > 0.5$ versus the effective surveyed time-volume for BNS mergers; the cumulative number of candidates is marked by the solid black line, while the blue line and the dark and light blue bands are the median and the 50% and 90% confidence intervals [15].

Sections 2 and 3 summarize the detections during O3a and O3b runs. Section 4 discusses their astrophysical implications of the detections. Section 5 provides the final remarks about the gravitational wave observations during O3.

2. O3a Detections

After an interval for upgrades of the interferometers, LIGO and Virgo began O3a run on 2019 April 1 and ended observations on 2019 October 1. Compared to O2 run, the duty cycle of the interferometer network improved, as the detection range, producing a larger detection rate (Fig. 1). The detections during O3a run have been reported in the GWTC-2 catalog [12], that contains 39 candidate gravitational wave events with a false alarm rate threshold of two per year, among them 26 previously reported in GCN Notices and Circulars. For comparison, the GWTC-1 catalog contained 11 events [6]. The majority of the events in GWTC-2 catalog are BBH mergers, spanning a range of total masses from about 14 $M_\odot$ to about 150 $M_\odot$ (GW190521, the first detected intermediate mass black hole), a larger interval compared to the GWTC-1 catalog [6] and including systems with largely asymmetric mass ratios (GW190412); both GW190412 and GW190521

will be discussed below. From the point of view of effective inspiral spins, 11 of the 39 events exhibit positive effective inspiral spin, while none of them show negative effective inspiral spin. The GWTC-2 catalog includes also events where one or two components could be neutron stars, discussed below: the second BNS merger GW190425 and GW190814, whose secondary could be either a neutron star or a black hole. The GWTC-2 catalog has been followed by the GWTC-2.1 catalog [14], reporting a deeper list of candidate events observed during O3a with a false alarm rate threshold of 2 per day. The GWTC-2.1 catalog added 8 candidates and reclassified 3 events with a low probability of astrophysical origin.

The masses of the O3a events reported in GWTC-2 catalog are shown in Fig. 2.

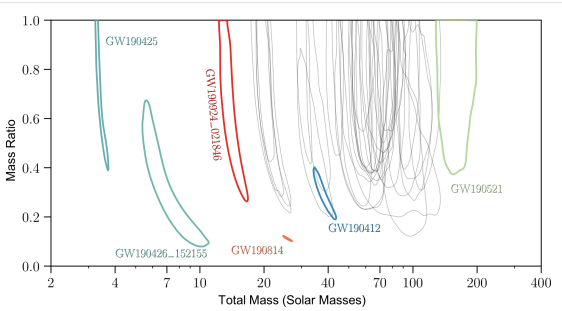

Figure 2: Estimates of mass ratio and total mass for all O3a events, with peculiar events highlighted [12].

2.1 GW190412

The BBH mergers detected during O1 and O2 runs involved binaries with components having similar masses [6]. The components of the GW190412 BBH merger [8] have asymmetric masses, m_1=30.1$^{+4.6}_{-5.3}$ $M_\odot$, m_2 = 8.3$^{+1.6}_{-0.9}$ $M_\odot$, with a mass ratio $q = m_2/m_1$ = 0.28$^{+0.12}_{-0.07}$. GW190412 is the first BBH merger showing higher multipoles of gravitational wave emission, while only the leading quadrupole order had been detected in previous mergers. The more massive black hole in GW190412 had a dimensionless spin magnitude in the range between 0.22 and 0.6.

2.2 GW190425

GW190425 is the second observed BNS merger [9], with component masses in the range from 1.12 to 3.52 $M_\odot$, consistent with the known masses of neutron stars. The total mass of GW190425, 3.4$^{+0.3}_{-0.1}$ $M_\odot$, is larger than the total mass of the most massive Galactic binary pulsar, 2.89 $M_\odot$ [25]. The possibility of a BBH merger cannot be excluded since there is no evidence of tidal deformability in the gravitational wave signal. Due to the poor sky localization (8284 deg^2) and the large distance (159$^{+69}_{-71}$ Mpc), there was no confirmed electromagnetic counterpart that could be associated to GW190425, with the possible exception of [33], that observed the weak Gamma Ray Burst GRB190425 a few seconds after the BNS merger, using the Anti-Coincidence Shield (ACS) of the gamma ray spectrometer SPI aboard the INTEGRAL observatory.

2.3 GW190521

The components of GW190521 [10] have masses $m_1 = 85^{+21}_{-14}$ $M_\odot$, $m_2 = 66^{+17}_{-18}$ $M_\odot$, with a total mass $M = m_1 + m_2 = 150^{+29}_{-17}$ $M_\odot$ and a remnant mass $m_f = 142^{+28}_{-16}$ $M_\odot$, making the remnant the first

detected Intermediate Mass Black Hole (IMBH). Intermediate mass black holes [27] are expected to have masses ranging from 10^2 to 10^5 $M_\odot$, between the regions of stellar mass black holes ($\leq 10^2$ $M_\odot$) [20, 24, 31] and of supermassive black holes ($\geq 10^5$ $M_\odot$) [34]. The mass of the heavier binary component in GW190521 has a high probability to be within the Pair-Instability SuperNova mass gap [35]. The massive black hole could have been formed in the merger of two light black holes, possibly in the accretion disk of an active galactic nucleus (AGN). In the assumption of a quasi-circular merger, the original black holes had high spins misaligned with respect to the orbital angular momentum, producing a precession of the orbital plane. A possible electromagnetic counterpart has been suggested by [26], after the observation by the Zwicky Transient Facility of a flare from AGN J124942.3+344929. The event can be explained by a kicked BBH merger in the accretion disk of the AGN, with a total mass of about 100 $M_\odot$, with the flare expected to reoccur when the merger remnant will cross again the disk [26].

2.4 GW190814

The components of GW190814 merger [11] had masses $m_1 = 23.2^{+1.1}_{-1.0}$ $M_\odot$, $m_2 = 2.59^{+0.08}_{-0.09}$ $M_\odot$. The mass of secondary lies in the low mass gap between 2.5 and 5 $M_\odot$ that separates neutron stars [32] from black holes [20, 24, 31]. While some theoretical Equations of State allow neutron star masses up to about 3 $M_\odot$ [30], the most massive Galactic pulsar has a mass of $2.14^{+0.10}_{-0.09}$ $M_\odot$ [23] and the GW170817 merger set an upper limit of 2.4 $M_\odot$ [2, 5]. While the mass of the primary object of GW190814 is consistent with the mass of stellar black holes, the mass of the secondary component suggests that it could be either the lightest black hole or the heaviest neutron star ever observed [11]. GW190814 could be interpreted as a NSBH detection, but there is no strong evidence for the secondary being a neutron star, since there are no observed tidal effects and there is no detected electromagnetic counterpart.

3. O3b detections

LIGO and Virgo began O3b run on 2019 November 1 and ended observations on 2020 March 27, because of COVID pandemic. The duty cycle and the detection range of the interferometer network improved, leading to a large detection rate (Fig. 1). The detections during O3b run have been reported in the GWTC-3 catalog, published after the HEASA conference [15]. The catalog contains 35 compact binary merger candidates with a probability of astrophysical origin $p_{astro} > 0.5$, among them 18 previously reported as low-latency public alerts [15]. Among O3b candidates, 32 are consistent with binary black hole mergers and 3 with neutron star-black hole (NSBH) mergers, the first detections of this class of events [18]. Two NSBH hole mergers will be discussed below [18]. The BBH mergers have total masses ranging from about 17.5 $M_\odot$ to about 148 $M_\odot$ [15]. The masses of the O3b events are reported in Fig. 3.

3.1 GW200105 and GW200115

The events GW200105 and GW200115 are the first detections of NSBH mergers [18], showing that all possible binaries formed by neutron stars and black holes are gravitational wave sources. NSBH mergers could be accompanied by electromagnetic emission [21], but the poor sky localization of the two candidates (7200 deg^2 for GW200105, 600 deg^2 for GW200115) and their large

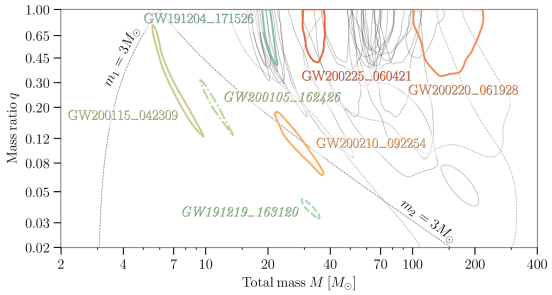

Figure 3: Estimates of mass ratio and total mass for all O3b events, with peculiar events highlighted [15].

distances (280^{+110}_{-110} Mpc for GW200105 and 300^{+150}_{-100} Mpc for GW200115) made observation of electromagnetic radiation unlikely and no counterpart was detected.

The component masses of GW200105 are $m_1 = 8.9^{+1.2}_{-1.5}$ $M_\odot$ and $m_2 = 1.9^{+0.3}_{-0.2}$ $M_\odot$, while for GW200115 are $m_1 = 5.7^{+1.8}_{-2.1}$ $M_\odot$ and $m_2 = 1.5^{+0.7}_{-0.3}$ $M_\odot$, respectively. In both mergers the heavier component is consistent with a black hole, while the lighter one is consistent with a neutron star. The estimates for the masses of the mergers are shown in Fig. 4.

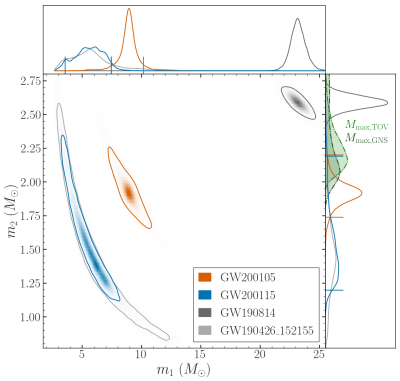

Figure 4: Mass of black holes against mass of neutron stars for GW200105 and GW200115 mergers [18]. The top and right panels summarize the information about mass of the black hole mass and of the nuetron star mass, respectively. The properties of the events GW190814 and GW190426_152155, a weak NSBH candidate, are also reported for comparison.

NSBH systems can be formed through two possible channels [29]. In the former a binary star system witnesses supernova explosions producing a black hole and a neutron star. In the latter the neutron star and the black hole are independently formed in supernova explosions and later form a binary system, a mechanism favoured in dense environments as globular clusters. The spin orientation of the black hole is preferably aligned with the orbit in the first formation path. While the black hole spin in GW200105 was not conclusive, the black hole spin in GW200115 was likely opposite to the orbit direction, suggesting the formation in a dense environment. The merger GW200105 has been later reclassified in the GWTC-3 catalog [15] due to its low p_{astro} value.

4. Astrophysical and Cosmological Implications

The mergers detected by LIGO-Virgo contribute to the study of the astrophysical populations of black holes and neutron stars. The detections in GWTC-1 catalog [6] suggested that less than 1% of BBH mergers could be associated to component masses above 45 $M_\odot$ and excluded large component spins aligned with the orbital angular momentum [7]. The detections in GWTC-2 catalog [12] suggested that the BBH population cannot be described by a power law only, but required the introduction of a new power law with different index or a peak in the region around 30-40 $M_\odot$ [13]. Some of the spins were misaligned with respect to the orbital angular momentum and produced precession [13], confirming the results of the GWTC-1 catalog [22]. The GWTC-2 confirmed the GWTC-1 suggestion that the BBH merger rate is increasing with redshift [13].

The population properties of the compact binary mergers detected through GWTC-3 have been reported by [17], that used observations with a false alarm rate < 0.25 yr^{-1}. The mass distribution of neutron stars extends up to $2.0^{+0.3}_{-0.2}$ $M_\odot$ [17], in contrast with the mass distribution of Galactic BNS. The observations confirm the presence of overdensities in the BBH mass distribution at masses of about 10 $M_\odot$ and 35 $M_\odot$ [17], possible signatures of the formation environment. The black hole mass distribution is suppressed between 2.1 $M_\odot$ and 5.8 $M_\odot$ [17], in agreement with the gap suggested by X-ray observations [28]. The majority of black holes has small spins, half of them less than 0.26, at least some of them showing spin-orbit misalignment. The BBH effective aligned inspiral spins is found to be correlated to the mass ratio. The rate of BBH mergers increases with redshift, confirming previous observations [13]. The rates of merger events have been updated for all classes of coalescences as 13-1900 Gpc^{-3} yr^{-1} for BNS, 7.4-320 Gpc^{-3} yr^{-1} for NSBH, 16-130 Gpc $^{-3}$ yr^{-1} for BBH.

The detections in the GWTC-3 catalog have been used to estimate the Hubble constant H_0 [19], combining the luminosity distance from the gravitational wave observations and the corresponding redshift estimated using either the redshifted masses or the GLADE+ galaxy catalog. The two methods produce estimates of $H_0=68^{+13}_{-7}$ km s^{-1} Mpc^{-1} and $H_0=68^{+8}_{-6}$ km s^{-1} Mpc^{-1}, respectively, improving previous limits set by the GWTC-2 detections [16].

5. Conclusions

The O3 run of the LIGO-Virgo Collaboration has produced a large number of detections, a total of 90 combined with the previous runs. The improved sensitivity during the O3 run has allowed to investigate regions of black hole masses never accessed before, with the detection of the first Intermediate Mass Black Hole and the observation of higher order modes beyond quadrupole. During O3 run the first NSBH coalescences have been observed, showing that all combinations of compact objects can form merging binaries, and an improved estimation of Hubble constant has been presented.

References

[1] B. P. Abbott et al., *PRL* **116** (2016) 061102.

[2] B. P. Abbott et al., *PRL* **119** (2017) 161101.

[3] B. P. Abbott et al., *ApJL* **848** (2017) L12.

[4] B. P. Abbott et al., *ApJL* **848** (2017) L13.

[5] B. P. Abbott et al., *PRL* **123** (2019) 011001.

[6] B. P. Abbott et al., *PRX* **9** (2019) 031040.

[7] B. P. Abbott et al., *ApJ* **882** (2019) L24.

[8] R. Abbott et al., *PRD* **102** (2020) 043015.

[9] B. P. Abbott et al., *ApJL* **892** (2020) L3.

[10] R. Abbott et al., *PRL* **125** (2020) 101102.

[11] R. Abbott et al., *ApJL* **896** (2020) L44.

[12] R. Abbott et al., *PRX* **11** (2021) 021053.

[13] R. Abbott et al., *ApJ* **913** (2021) L7.

[14] R. Abbott et al., arXiv:2108.01045.

[15] R. Abbott et al., arXiv: 2111.03606.

[16] R. Abbott et al., *ApJ* **909** (2021) 218.

[17] R. Abbott et al., arXiv:2111.03634.

[18] R. Abbott et al., *ApJL* **915** (2021) L5.

[19] R. Abbott et al., arXiv:2111.03604.

[20] C. D. Bailyn et al., *ApJ* **499** (1998) 367.

[21] E. Berger, *ARA&A* **52** (2014) 43.

[22] S. Biscoveanu et al., *PRL* **126** (2021) 17.

[23] H. Cromartie et al., *NatA* **4** (2019) 72.

[24] W. M. Farr et al., *ApJ* **741** (2011) 103.

[25] N. Farrow et al., *ApJ* **876** (2019) 18.

[26] M. Graham et al., *PRL* **124** (2020) 251102.

[27] J. E. Greene et al., *ARA&A* **58** (2020) 257.

[28] L. Kreidberg et al., *ApJ* **757** (2012) 36.

[29] I. Mandel and F. S. Broekgaarden, arXiv:2107.14239.

[30] H. Müller and B. D. Serot, *NuP A* **606** (1996) 508.

[31] F. Ozel et al., *ApJ* **725** (2010) 1918.

[32] F. Ozel et al., *ApJ* **757** (2012) 55.

[33] A. S. Pozanenko et al., *AstL* **45** (2020) 710.

[34] M. Volonteri, *A&AR* **18** (2010) 279.

[35] S. E. Woosley, *ApJ* **836** (2017) 244.